

Isotropic and Uniaxial Strain Induced Band Modulation of PbTe

Xiaoguang Wang^{1, a}, Yazhou Sun^{1, b}, Liangming Peng^{1, c}

¹CAS Key Laboratory for Mechanical Behavior and Design of Materials, Department of Modern Mechanics, School of Engineering Science, University of Science and Technology of China, Hefei 230026, PR China

^aemail:wang2006@mail.ustc.edu.cn, ^bemail:yzsun@mail.ustc.edu.cn, ^cemail:penglm@ustc.edu.cn

Keywords: Strain; PbTe; First principles calculation; band structure

Abstract. First principles calculations were performed to explain the deformation feature and band gap variation behavior of PbTe under isotropic and uniaxial strain along [100], [110] and [111] directions. Calculations showed that the band gap variation regularity is quite different between the first and the last two cases due to the different lattice deformation modes. The introduction of shearing strain may significantly reduce the band gap of PbTe, and therefore the band structure of PbTe can be modulated by introducing proper strain.

Introduction

Thermoelectric (TE) materials have been attracted extensive attentions in the past two decades because of the realization of direct and environmental friendly conversion between heat energy and electronic power [1]. Generally, the performance of TE materials is determined by the dimensionless figure of merit $ZT = S^2\sigma T/\kappa$, where S , σ , T and κ are the Seebeck coefficient, electrical conductivity, absolute temperature and thermal conductivity, respectively. Accordingly, increasing the power factor, $PF = S^2\sigma$, is essential to enhancing ZT [2-4]. Furthermore, the two related parameters, S and σ , are both depended on the band structure [5].

Recently, strain engineering has been proved to be effective in tuning the band structure of many materials such as Bi_2Te_3 , Sb_2Te_3 , $\text{Bi}_2\text{O}_2\text{Se}$, $\text{La}_2\text{NiO}_{4+\delta}$ and SrTiO_3 to improve their TE properties [6-9]. Besides, this strain (ε) effect has been also observed in lead telluride, which is one of the most potential and widely studied TE materials. Several studies have shown that the band gap of PbTe can be shifted by thermal or pressure induced strain [10-12] and the latter could even lead to a band inversion and topological phase transition [13, 14]. However, such discussions on the band structure-strain relationship of PbTe are merely focused on the isotropic strain. PbTe is usually doped or designed into multiphase structures or 2D thin films to achieve better TE performance. Therefore, the actual strain or deformation conditions are far more complicated in most cases due to the heterogeneous doping and lattice mismatch [15-18]. In this contribution, discussions will be presented mainly dealing with the lattice deformation peculiarity and band structure evolutionary behavior of PbTe under different types of strain.

Computational details

First principles calculations were performed using the projector augmented wave (PAW) [19] method and GGA-PBE exchange-correlation functional [20] as implemented in VASP [21]. Herein, discussions were focused on the tensile and compressive isotropic strain and uniaxial strain along [100], [110], [111] directions in PbTe. These strains were introduced basing on the conventional cell of PbTe with optimized lattice constant of $a_0=6.559 \text{ \AA}$. The magnitude of strain was increased gradually in step of 1%. Our calculations used 300 eV plane wave cutoff energy and $11\times 11\times 11$ Monkhorst-Pack k -point sampling in the first Brillouin zone (BZ). The total energy converged within 1×10^{-5} eV and the interatomic forces were less than 0.01 eV/\AA in all fully relaxed structures. The well known spin-orbit coupling (SOC) effect was included in all calculations except the structural relaxation since it almost exerts no influence on the structural optimization [17, 22].

Results and discussions

Unstrained PbTe

To begin with, some of the important features such as crystal and band structures of unstrained PbTe are summarized. PbTe normally exhibits a NaCl-type face-centered (*fcc*) structure with lattice constant of $a=b=c=a_0$ and edge angle of $\alpha=\beta=\gamma=90^\circ$. In the simple cubic BZ of the conventional cell, both the valence band maximum (VBM) and conduction band minimum (CBM) exist at the \mathbf{R} point and generate a direct band gap (E_g). The calculated E_g is 0.077 eV, which consists well with the previously calculated results [22, 23].

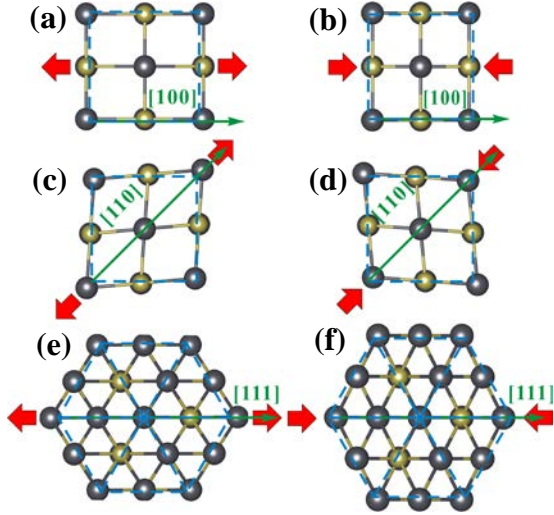


Fig. 1. Relaxed structures of PbTe with 10% tensile and compressive strain along [100], [110] and [111] directions. Unstrained lattice is given by dashed lines.

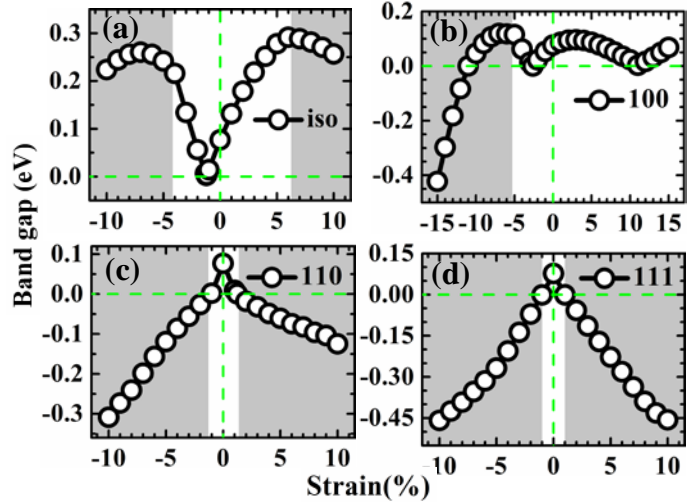


Fig. 2. The band gap variation of PbTe with the strength of (a) isotropic strain and uniaxial strain along (b) [100], (c) [110] and (d) [111] directions. Band gaps in grey areas are indirect ones.

Structural evolution

PbTe with isotropic strain maintains the *fcc* symmetry during the deformation. However, as illustrated in Fig. 1, situations under uniaxial strains are more complex. It is reasonable that tensile strain along [100] direction induces a reduction of b and c because of the Poisson effect, whereas it behaves just oppositely in compressive condition (cf. Figs. 1 (a) and (b)). In these two cases, the three orthogonal directions, a , b and c , remain mutually perpendicular during the deformation, resulting in a cubic-tetragonal lattice transition trend.

Fig. 1 (c) depicts the relaxed structure with tensile strain along [110] direction. In this case, both a and b are elongated whereas c is decreased. Furthermore, the original right angle γ is reduced significantly. Again, the compressive strain produces an opposite effect (Fig. 1 (d)). In comparison, the [111] directional strain induces more symmetric lattice deformation. Concretely, the tensile strain results in a lattice constant of $a=b=c>a_0$ and edge angle of $\alpha=\beta=\gamma<90^\circ$ while compressive strain leads to $a=b=c<a_0$ and $\alpha=\beta=\gamma>90^\circ$, as evident in Figs. 1 (e) and (f). Nevertheless, such angle change (shearing strain) does not exist in the isotropically and [100] directionally strained conditions although the lattice constants change similarly.

Band structure

Fig. 2 shows the strain-dependence of band gap in PbTe. E_g increases firstly and then decreases with the increase of isotropic tensile strain and the maximum value of 0.292 eV occurs at $\varepsilon=6\%$ (Fig. 2 (a)). It is worth noting that a direct-to-indirect band gap transition is observed for $\varepsilon>6\%$. This is mainly attributed to the down-shift of the light \mathbf{L} band and the slight up-shift of the heavy $\mathbf{\Sigma}$ band, inducing the convergence of valence band that is beneficial to the thermoelectric performance of PbTe [24, 25]. In compressive condition, E_g is decreased at first and then closed at $\varepsilon\approx-1.20\%$.

Intriguingly, the band gap is reopened and increased with further increasing the compressive strain. The observed phenomena are consistent well with the band gap variation regularity of PbTe under pressure [11, 12, 26]. It should be noted that the band gap becomes indirect for $\varepsilon < -4\%$ and E_g begins to decrease again for $\varepsilon < -7\%$.

From Fig. 2 (b), it can be seen that the band gap of PbTe with [100] uniaxial strain changes in a similar trend to that under isotropic condition in the strain region of $-10\% \leq \varepsilon \leq 10\%$. However, tensile strain did not lead to indirect band gap transition and E_g varied more gently in the former. The similarity might be originated from the deformation similitude that only linear strain were introduced in both cases. It is worth noting that the band gap can be closed when [100] tensile strain reaches 11% and reopened by further increase the strain magnitude. However, E_g continues to reduce after reaching its maximum value of 0.120 eV at $\varepsilon = -7\%$ in the compressive condition and reclosed at $\varepsilon = -11\%$. Moreover, the CBM and VBM overlaps for $\varepsilon < -11\%$, resulting in negative band gaps and a metal transition. Accordingly, the change of band gap with strain exhibits strong tension-compression asymmetry under the isotropically and [100] directionally strained conditions.

As shown in Figs. 2 (c) and (d), quite different band gap changing regularities were observed under [110] and [111] directionally strained conditions due to the shearing strain. In both cases, E_g decreases monotonously with the increase of tensile and compressive strain. The band gap is closed at $\varepsilon = 1.23\%$ and -1% in the [110] case and the corresponding values are $\pm 1\%$ in [111] condition. After the closure, the valence and conduction bands are overlapped and indirect negative band gaps are generated. Please note that the [111] directional strain induced variation of E_g are almost the same in tensile and compressive cases. The aforementioned symmetric lattice deformation should be responsible for this tension-compression symmetry of the band gap variation.

Conclusions

In summary, the deformation peculiarity and band gap variation behavior of PbTe under isotropic and typical uniaxial strain were investigated by first principles calculations. The preliminary results reveal that the lattice edge angle of PbTe can be changed by [110] and [111] directional linear strain, and thus shearing strain is introduced. Due to the lattice distortion, the band gap decreases monotonously with increasing tensile and compressive strain, which is completely different from that in the isotropically and [100] uniaxially strained conditions. However, band gap closure is observed in all cases. Accordingly, the lattice deformation type is dominant in modulating the band structure of PbTe. Therefore, one may tune the band structure of such materials intentionally by introducing proper strain to achieve higher ZT for practical applications.

Acknowledgements

Authors thank the Supercomputing Center (SCC) of University of Science and Technology of China (USTC) for the computing facility supports.

References

- [1] L.E. Bell. Cooling, heating, generating power, and recovering waste heat with thermoelectric systems [J]. Science, 2008 321 (5895) 1457-1461.
- [2] M. Zebarjadi, K. Esfarjani, Z.X. Bian, et al. Low-Temperature Thermoelectric Power Factor Enhancement by Controlling Nanoparticle Size Distribution [J]. Nano Letters, 2011 11 (1) 225-230.
- [3] J.H. Bahk, P. Santhanam, Z.X. Bian, et al. Resonant carrier scattering by core-shell nanoparticles for thermoelectric power factor enhancement [J]. Applied Physics Letters, 2012 100 (1) 012102.
- [4] B. Paul, P.K. Rawat, P. Banerji. Dramatic enhancement of thermoelectric power factor in PbTe:Cr co-doped with iodine [J]. Applied Physics Letters, 2011 98 (26) 262101.
- [5] J.R. Sootsman, D.Y. Chung, M.G. Kanatzidis. New and Old Concepts in Thermoelectric

- Materials [J]. *Angewandte Chemie-International Edition*, 2009 48 (46) 8616-8639.
- [6] D. Zou, Y. Liu, S. Xie, et al. Effect of strain on thermoelectric properties of SrTiO₃: First-principles calculations [J]. *Chemical Physics Letters*, 2013 586 159-163.
- [7] V. Pardo, A.S. Botana, D. Baldomir. Strain effects to optimize thermoelectric properties of hole-doped La₂NiO_{4+δ} via ab initio calculations [J]. *Physical Review B*, 2013 87 (12) 125148.
- [8] D. Guo, C. Hu, Y. Xi, et al. Strain Effects To Optimize Thermoelectric Properties of Doped Bi₂O₂Se via Tran–Blaha Modified Becke–Johnson Density Functional Theory [J]. *The Journal of Physical Chemistry C*, 2013 117 (41) 21597-21602.
- [9] N.F. Hinsche, B.Y. Yavorsky, I. Mertig, et al. Influence of strain on anisotropic thermoelectric transport in Bi₂Te₃ and Sb₂Te₃ [J]. *Physical Review B*, 2011 84 (16) 165214.
- [10] J.W. Tomm, L. Werner, D. Genzow, et al. Experimental evidence of strain-induced gap shifts in PbTe epitaxial layers by photoluminescence [J]. *Physica Status Solidi (a)*, 1988 106 (2) 509-514.
- [11] Y.L. Yang. Elastic moduli and band gap of PbTe under pressure: ab initio study [J]. *Materials Science and Technology*, 2012 28 (11) 1308-1313.
- [12] L.Q. Xu, Y.P. Zheng, J.C. Zheng. Thermoelectric transport properties of PbTe under pressure [J]. *Physical Review B*, 2010 82 (19) 195102.
- [13] P. Barone, T. Rauch, D. Di Sante, et al. Pressure-induced topological phase transitions in rocksalt chalcogenides [J]. *Physical Review B*, 2013 88 (4) 045207.
- [14] W. Feng, W. Zhu, H.H. Weiering, et al. Strain tuning of topological band order in cubic semiconductors [J]. *Physical Review B*, 2012 85 (19) 195114.
- [15] K. Biswas, J.Q. He, Q.C. Zhang, et al. Strained endotaxial nanostructures with high thermoelectric figure of merit [J]. *Nature Chemistry*, 2011 3 (2) 160-166.
- [16] K. Biswas, J.Q. He, I.D. Blum, et al. High-performance bulk thermoelectrics with all-scale hierarchical architectures [J]. *Nature*, 2012 489 (7416) 414-418.
- [17] X.G. Wang, J. Liu, L.M. Peng. First-principles investigation of dual substitutional impurity-induced electronic structural modulation of PbTe on cationic and anionic sites [J]. *Acta Materialia*, 2013 61 (17) 6428-6442.
- [18] R. Leitsmann, F. Bechstedt. Electronic-structure calculations for polar lattice structure mismatched interfaces: PbTe/CdTe(100) [J]. *Physical Review B*, 2007 76 (12) 125315.
- [19] P.E. Blochl. PROJECTOR AUGMENTED-WAVE METHOD [J]. *Physical Review B*, 1994 50 (24) 17953-17979.
- [20] J.P. Perdew, K. Burke, M. Ernzerhof. Generalized Gradient Approximation Made Simple [J]. *Physical Review Letters*, 1996 77 (18) 3865-3868.
- [21] G. Kresse, J. Furthmuller. Efficient iterative schemes for ab initio total-energy calculations using a plane-wave basis set [J]. *Physical Review B*, 1996 54 (16) 11169-11186.
- [22] Y. Zhang, X.Z. Ke, C.F. Chen, et al. Thermodynamic properties of PbTe, PbSe, and PbS: First-principles study [J]. *Physical Review B*, 2009 80 (2) 024304.
- [23] K. Hoang, S.D. Mahanti, M.G. Kanatzidis. Impurity clustering and impurity-induced bands in PbTe-, SnTe-, and GeTe-based bulk thermoelectrics [J]. *Physical Review B*, 2010 81 (11) 115106.
- [24] Y. Pei, X. Shi, A. LaLonde, et al. Convergence of electronic bands for high performance bulk thermoelectrics [J]. *Nature*, 2011 473 (7345) 66-69.
- [25] L.D. Zhao, H.J. Wu, S.Q. Hao, et al. All-scale hierarchical thermoelectrics: MgTe in PbTe facilitates valence band convergence and suppresses bipolar thermal transport for high performance [J]. *Energy & Environmental Science*, 2013 6 (11) 3346-3355.
- [26] A. Svane, N.E. Christensen, M. Cardona, et al. Quasiparticle self-consistent GW calculations for PbS, PbSe, and PbTe: Band structure and pressure coefficients [J]. *Physical Review B*, 2010 81 (24) 245120.